1.3   CIRRUS CLOUD AND POLAR STRATOSPHERIC CLOUD MEASUREMENTS FROM CALIPSO

M. Patrick McCormick[1], Hovakim Nazaryan[1], and Michael T. Hill[1]

[1]The Center for Atmospheric Sciences, Hampton University, Hampton, Virginia

ABSTRACT

Using the first year of the Cloud-Aerosol Lidar and Infrared Pathfinder Satellite Observations (CALIPSO) data, a study of the global and seasonal distribution of cirrus clouds, that have been identified as one of the most uncertain components in weather and climate studies, and of Polar Stratospheric Clouds (PSCs), important as sites for heterogeneous chemistry and polar ozone loss, have been conducted. Few instruments can deduce the global presence of cirrus clouds, especially sub-visual clouds and those of low optical thickness. Similarly, few remote sensors can produce the vertical and spatial distribution of PSCs each day over the local winter and early spring periods. Satellite lidar has the ability to profile multi-layer cloud structures and it is particularly useful for the detection of sub-visible cirrus, and PSCs over the poles where CALIPSO's coverage is the most spatially dense. satellite mission provides comprehensive observations of cloud vertical structure on a near global scale. We investigate the latitude-longitude and vertical distributions of PSCs and cirrus, and thickness of cirrus clouds. In addition, we classify PSCs by type (solid/liquid nitric acid and water ice) using the depolarization ratio and backscatter ratio from CALIOP at 532 nm wavelength, and GMAO temperature data. For example, our investigation of top-layer cirrus clouds shows maximum occurrence frequency of up to 70% near the tropics at the 100° - 180° longitude band.

Corresponding author address: M. Patrick McCormick, The Center for Atmospheric Sciences, Hampton University, Hampton, Virginia, 23668, e-mail: pat.mccormcik@hamptonu.edu

We also analyze the seasonal behavior of the cirrus cloud frequency. Our results show large latitudinal movement of cirrus cloud cover with the changing seasons. Obviously, PSCs have a much higher frequency of occurrence over Antarctica in winter than over the Arctic. This paper will describe and characterize the global distribution of cirrus clouds and PSCs and compare these data with previously published data sets.

1. INTRODUCTION

Cirrus clouds play a significant role in the energy budget of the earth–atmosphere system by their effects on the transfer of radiant energy through the atmosphere (Hansen et al., 1997). Unlike many low clouds that have a cooling effect on solar radiation through scattering, high thin cirrus clouds scatter only a small amount of solar radiation and prevent a large quantity of long-wave radiation from leaving the earth–atmosphere system (Liou, 1986).

Cirrus clouds normally exist in the upper troposphere and sometimes extend into the stratosphere. Cirrus clouds are globally distributed and are composed almost exclusively of non-spherical ice crystals (see Wylie and Menzel, 1999; Wylie et al., 1994; Rossow and Schiffer, 1999). The Geoscience Laser Altimeter System (GLAS) data, carried on board the Ice, Cloud, and land Elevation Satellite (ICESat) (Spinhirne et al., 2005), showed that maxima in thin near-tropopause cirrus (TNTC) tend to occur over regions of intense convective activity like equatorial Africa and South America, where vigorous continental convection occurs, and in the western Pacific, where significant oceanic convection occurs (Dessler et al., 2006).

Several investigations on the development of cirrus cloud climatologies have been accomplished recently. A number of field

campaigns have been dedicated to elucidate cirrus cloud properties like the First International Satellite Cloud Climatology Project (ISCCP) Regional Experiment (FIRE) (see Starr, 1987), and the Subsonic Aircraft: Contrail and Cloud Effects Special Study (SUCCESS) (Toon and Miake-Lye, 1998).

In this work we also study Polar Stratospheric Clouds (PSCs) (McCormick et al., 1982). PSCs provide surfaces for heterogeneous chemical reactions to convert chlorine and bromine reservoir species into gaseous molecular forms that catalytically destroy ozone through photolysis. In addition, these heterogeneous reactions tend to reduce the concentrations of nitrogen dioxide (NO_2), which inhibits the transformation of chlorine back into its reservoir state (Solomon et al., 1986; Solomon, 1999). Thus, the presence of PSCs is an important factor in high latitude ozone depletion during late winter and early spring when sunlight returns to the polar region. There are three main classifications of PSCs based on particle composition (Poole and McCormick, 1988; Browell et al., 1990; Toon et al., 1990). PSC particles can consist of solid nitric acid trihydrate crystals (type 1a), supercooled liquid ternary solution (H_2SO_4-HNO_3-H_2O) droplets (type 1b), or water ice (type 2). The type 1 PSCs can precipitate ozone destruction by reducing the amount of nitric acid in gaseous state during the formation of the cloud or by removing nitrogen from the region altogether through the sedimentation of large particles (Toon et al., 1986; Solomon, 1999). Additionally, the type 1 PSCs can form at temperatures above the frost point, facilitating ozone destruction at higher temperatures than the type 2 PSCs.

Satellite remote sensing is the only practical means of observing cloud and climate variables such as aerosols on a global scale. However, most satellite analysis only sample the optically thick and usually highest altitude clouds and it is difficult to determine from satellite imagery how deep a cloud extends into the atmosphere regardless of its optical depth (Wang et al., 1996). Satellite lidar has the ability to profile multi-layer cloud structures on a global scale, spatially and temporally, and it is particularly useful for the detection of subvisual cirrus. With passive sensors, it is difficult to detect thin cirrus clouds (optical depth less than 0.4), and as a result there are few quantitative,

global analyses of them (Dessler and Yang, 2003; Dessler et al., 2006). Woodbury and McCormick (1983) reported the spatial extent and frequency of cirrus clouds analyzed from the solar occultation SAGE extinction data over a 15-month period extending from February 1979 to April 1980. The analysis separates cirrus cloud observations into cirrus and thin cirrus based on the observed extinction values from the satellite experiment. Woodbury and McCormick (1986) extended their analysis to cover the time period from February 1979 to November 1981 and to provide zonally-averaged cirrus cloud cover and a cirrus global distribution.

However the Cloud-Aerosol Lidar and Infrared Pathfinder Satellite Observations (CALIPSO) satellite mission provides comprehensive observations of cloud vertical structure on a near global scale (Winker et al, 2003). CALIPSO was developed within the framework of collaboration between NASA, France's Centre National d'Etudes Spatiales (CNES), and Hampton University (Winker et. al, 2003; McCormick, 2002, 2004), and was launched on April 28, 2006 into a sun-synchronous 705-km circular polar orbit with an ascending node equatorial crossing time of 13:30 local time. Further, and importantly, CALIPSO flies in formation as part of the A-Train constellation, which consists of the Aqua, Aura, CALIPSO, CloudSat, and PARASOL satellites. The CALIPSO orbit is controlled to provide a space-time near coincidence with measurements from the other satellites of the constellation.

The CALIPSO payload consists of three nadir-viewing instruments: the Cloud-Aerosol Lidar with Orthogonal Polarization (CALIOP), the French-built Imaging Infrared Radiometer (IIR) and the Wide Field Camera (WFC). CALIOP is a three-channel lidar system (1064 nm and 532 nm parallel and perpendicular) with a 1 m receiving telescope (McCormick, 2004). The WFC provides meteorological context for the lidar measurements and is used during daytime only. The CALIPSO data products are archived with a vertical resolution of 30 m from 0 to 8 km, and 60 m from 8 to 20 km.

The objective of this study is to use data provided by CALIOP on CALIPSO to investigate the occurrence frequency and geometrical thickness of cirrus clouds on a near global scale,

and to classify Polar Stratospheric Clouds based on their optical properties.

Wylie and Menzel (1999) compiled the frequency and location of high-cloud observations from 1989 through 1997 using multi-spectral High Resolution Infrared Radiation Sounder (HIRS) data from the National Oceanic and Atmospheric Administration (NOAA) polar-orbiting satellites. Their study showed that clouds with optical depths greater than 0.1 cover 69% of the earth between 65 N and 65 S. High clouds were found more often in the tropics than in the northern and southern mid-latitudes.

During our investigation of cirrus clouds, we study clouds with Cloud Layer Base (CLB) altitude higher than 8 km in the tropics (15° S - 15° N) and higher than 5 km in the extratropics (see Eguchi et al., 2007). The geometric thickness of clouds under consideration is less than 8 km, and the Integrated Volume Depolarization Ratio (VDR) is greater than 0.2 (greater than 20%) to consider clouds mostly composed of non-spherical ice crystals. We define the cloud occurrence frequency as the ratio of the number of retrieved cirrus cloud layers to total number of observations by CALIOP. During our analysis we employ the 5 km layer (horizontal grid) CALIPSO cloud product.

We investigate the occurrence frequency and thickness of cirrus clouds measured by CALIOP as a function of time, latitude, and altitude (Wang et al., 1996; Wylie and Menzel, 1999). In particular, we examine the latitude-longitude distributions of cirrus clouds, including their seasonal behavior.

2. HORIZONTAL DISTRIBUTION OF CIRRUS CLOUD FREQUENCY.

Horizontal cloud cover is very important in the radiation field of the earth-atmosphere system and, hence, in weather and climate processes. To investigate the zonal variability to cloud occurrence, the CALIOP measurements are grouped into 10° latitude by 24° longitude bins. Our calculations of cirrus cloud occurrence frequency take into account only the top-layer clouds and obtain the cirrus cloud occurrence frequency distribution for single-layer clouds (see Figure 1) using the following formula:

$$Single\,Layer\,Frequency = \frac{N_S}{N_T} \cdot 100\% \,,$$

where N_S is the number of the retrieved top-layer cirrus clouds, and N_T is the number of total observations. Next we calculate the average frequency for each 10° latitude and 24° longitude bin as shown in Figure 1. Our results show maximum occurrence frequency of up to 70% of top-layer cirrus clouds near the tropics over the 100° – 180° E longitude band.

CALIOP is capable of retrieving multi-layer clouds, thus revealing the vertical structure of cirrus cloud distributions. Thus during our analysis we take into account not only the top-level clouds, but also the lower-level, overlapped cirrus clouds. We define the cloud occurrence frequency for multi-layer clouds as the ratio of the number of all retrieved cirrus cloud layers to total number of observations by CALIOP.
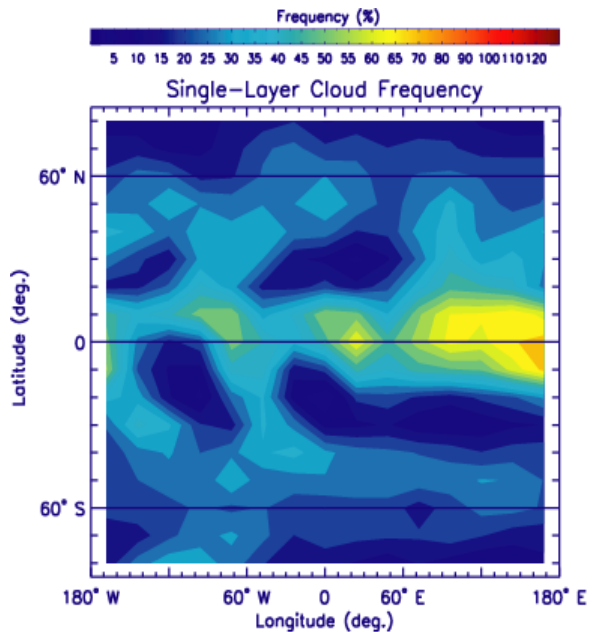
Figure 1. Latitude-Longitude distribution of the CALIOP cirrus cloud occurrence frequency over the period June 2006 to June 2007 for single-layer clouds.

For the multi-layer clouds, the cirrus occurrence frequency may be higher than 100%, since individual lidar returns may provide

information about multiple layers of clouds within each lidar profile. We obtain maximum occurrence frequency of multi-layer cirrus clouds of up to 130% in the latitude band 20° S to 20° N over the 100° – 180° E longitude band.

To examine the seasonal behavior of the cloud frequency distributions, CALIOP data are further grouped according to season. Figure 2 shows seasonal variations of the latitude – longitude distributions of the CALIOP cirrus cloud occurrence frequency for single-layer (top-level) clouds from June 2006 to May 2007. For June – August (northern summer), figure 2 shows high frequency of cirrus clouds up to ~80% from 10° S to 25° N latitude over 60° -

180° E longitude bands. This maximum frequency of occurrence moves south from September through the southern summer of December – February, where the maximum extends poleward to only about 15° S, much less than its north poleward extent in northern summer. The latitudinal movements of the maximum occurrence of cirrus clouds near the tropics are in agreement with the seasonal shift of the ITCZ.

There were several studies of the seasonal variation of cirrus clouds using passive remote sensors on a global scale. Wang et al. (1996) developed a climatology of cloud occurrence frequency based on the solar
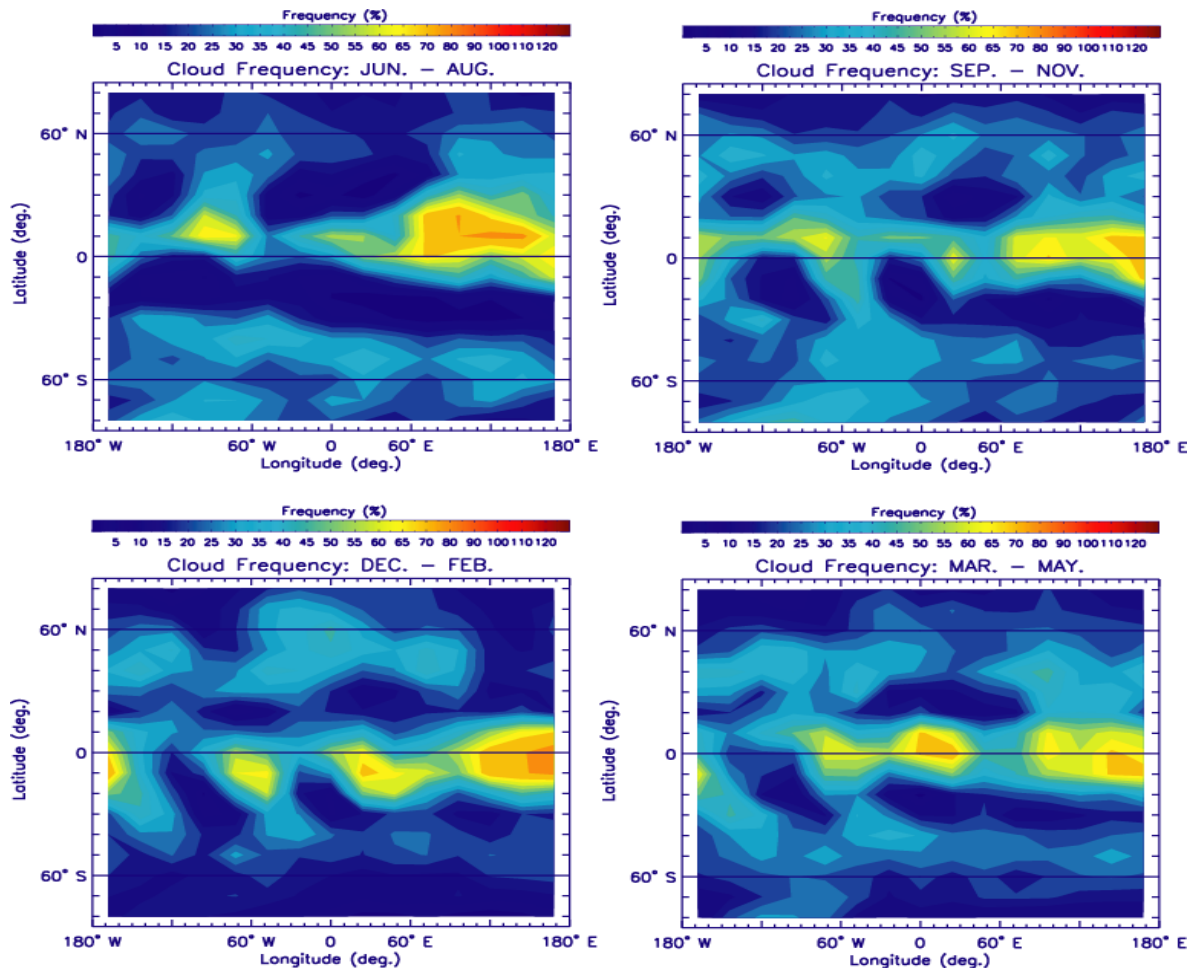
Figure 2. *Seasonal variations of the Latitude-Longitude distributions of the CALIOP cirrus cloud occurrence frequency of the top-layer clouds from June 2006 to May 2007.*

occultation observations of the Stratospheric Aerosol and Gas Experiment (SAGE) II between

1985 and 1990. They examined the seasonal variations of zonal mean cloud occurrence and

reported that the cloud occurrence in the subtropical regions has a distinct seasonal variation, with the maximum frequency in local summer and the minimum during local winter.

We also analyze the vertical distribution of occurrence frequency of the cirrus cloud top altitudes observed by CALIOP. Averaging over a year of data and all longitudes, the maximum of cirrus top altitude occurrence frequency in the 20° N – 20° S latitude band is about 13 % at 16 km.

## 3. DISTRIBUTION OF THE CIRRUS CLOUD THICKNESS.

We study the cirrus cloud geometrical thickness measured by CALIOP as a function of latitude and longitude. Cirrus cloud height and thickness are among the fundamental cloud parameters required for climate studies (Liou, 1986).

We calculate the latitude-longitude distribution of cirrus cloud thickness by averaging the thickness of the observed clouds for every 5° latitude and 10° longitude bin over the June 2006 – June 2007 period. Our results show that the average thickness of cirrus clouds is generally between 1.5 and 1.9 km in the majority of latitude-longitude bins. We also observe a concentration of relatively thicker clouds poleward of 70° S in the Antarctic with an area of peak thickness of about 2.3 km in the 60° - 120° E longitude band.

4. POLAR STRATOSPHERIC CLOUDS.

Data from the CALIOP lidar on CALIPSO are used to discriminate between these cloud types based on their optical properties (e.g., Browell et al., 1990). Since CALIOP includes two orthogonal polarization channels at the 532 nm wavelength, the depolarization ratio of the attenuated backscatter data (ratio of the perpendicular channel to the parallel channel) can be calculated. The backscatter ratio (ratio of the total attenuated backscatter to the molecular backscatter) at 532 nm wavelength can also be calculated using ancillary GMAO temperature and pressure data included in the CALIPSO data product and the molecular scattering cross section (Hostetler et al., 2006; Pitts et al., 2007).

Since PSCs form in the wintertime polar stratosphere, only CALIPSO data taken during June – August poleward of 60° S latitude, and during December - February poleward of 60° N latitude, between 15 – 25 km altitude are analyzed. Also, only the data from nighttime orbits, which have better signal to background noise characteristics than data from daytime orbits, are considered. The data from the CALIPSO profiles of each orbit are first separated into 1° latitude by 1° longitude by 1 km altitude bins. A minimum 532 nm backscatter coefficient threshold of 1×10^{-4} km^{-1} sr^{-1} and a maximum temperature of 195 K are used to filter the data. A PSC is considered to be detected only if the backscatter ratio is between 1.2 and 8.0, or if the backscatter ratio is greater than 8.0 and the depolarization ratio is greater than 0.05.
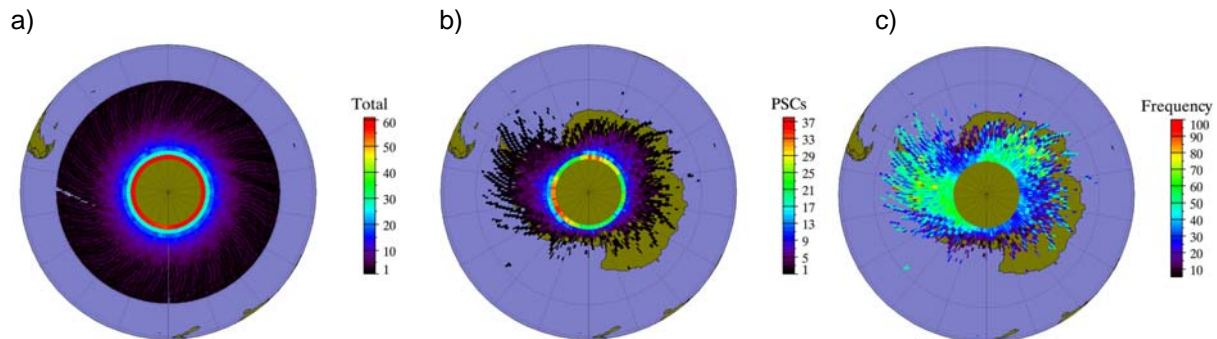

Figure 3. *Polar stratospheric cloud (PSC) measurement frequency by CALIPSO over Antarctica during August 2006. Plot a) shows the total number of measurements (orbits) made by CALIPSO every 1° latitude by 1° longitude. Plot b) shows the number of PSCs detected. Plot c) shows the relative frequency of PSCs detected by CALIPSO.*

5

At least 50% of the data points in a given bin must meet these criteria for a PSC to be considered present at that location. Finally, statistics are collected for each orbit, and a PSC is considered to be present in a given latitude and longitude bin if it is detected at any altitude between 15 – 25 km.

Figure 3 shows the results obtained over Antarctica during August 2006. Figure 3a gives the total number of orbits in which a measurement was made in a given bin. Figure 3b illustrates the number of orbits in which a PSC was detected in a given bin. Figure 3c shows the PSC measurement frequency. Note that the total number of measurements by latitude increases sharply toward the pole up to a latitude of about 82° S (see also Pitts et al., 2007). CALIPSO's orbital inclination prevents any nadir measurements from being made poleward of about 82° S and forces its orbital tracks to converge more densely around this ring where up to 60 measurements are made during the month. Because far fewer measurements are made at lower latitudes, the frequency statistics have a less reliable interpretation there. In general, more PSCs are observed over the Antarctic peninsula below South America, and between 0 - 20° E longitude, than over other regions of Antarctica.
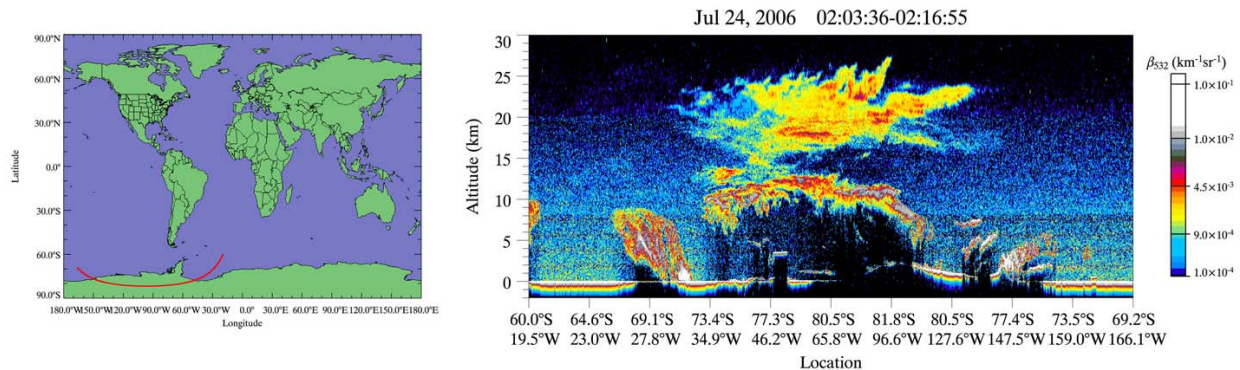

Figure 4. Total attenuated backscatter coefficient at 532 nm wavelength for a section of CALIPSO's orbit on July 24, 2006 over Antarctica. The plot on the left shows the orbital track of CALIPSO. The satellite is travelling to the west.

Figure 4 shows the total attenuated backscatter data at 532 nm wavelength for a section of CALIPSO's orbit on July 24, 2006. The left plot shows the orbital track of CALIPSO. The right plot shows relatively high values of the backscatter ($> 9{\times}10^{-4}$ km^{-1} sr^{-1}) between 15 – 25 km over the western edge of Antarctica where the PSC is. The PSC is classified according to the backscatter ratios and depolarization ratios of the data points. If the backscatter ratio is between 1.2 and 8.0 then it is considered a type 1 PSC. If the depolarization ratio of a type 1 PSC is greater than 0.05 then it is a type 1a, and if the depolarization ratio of a type 1 PSC is between 0.0 - 0.05 then it is a type 1b. It is considered a type 2 PSC if the backscatter ratio is greater than 8.0 and the depolarization ratio is greater than 0.05.

Figure 5 shows the results of the classification at the full resolution. In the figure, the color bar applies only to the region outside the altitude range 15 – 25 km. Within the 15 – 25 km altitude range four colors are used to indicate the status of the PSC type. Blue is used to indicate a type 1a PSC, red indicates a type 1b PSC, and green represents a type 2 PSC. White is used to illustrate that no PSC has been detected. This particular PSC appears to be predominantly type 2, although indications of a type 1 appear around the edges. In figure 6, a smoothing algorithm was applied to the data prior to classification. Each data point was replaced by the median of all data points within a box that included 31 profiles horizontally and 1/3 km altitude vertically, centered on the data point. The figure strongly indicates the presence of a type 1a PSC on the eastern edge of the cloud region (to the left in the plot). It also indicates a substantial region to the west (right) that could be a type 1b. This region is not evident in Figure 5.
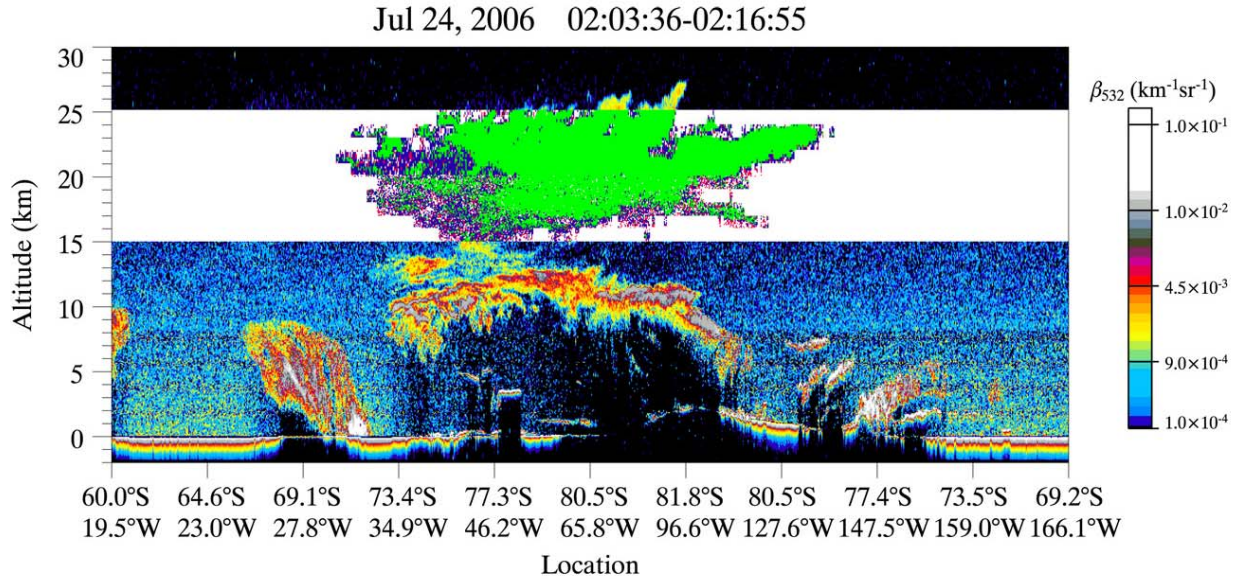
Figure 5. *Classification of PSC by composition for the same orbital section of CALIPSO as in Figure 4 (full resolution). Between 15-25 km, the color blue indicates type 1a, red indicates type 1b, and green indicates type 2 PSC.*
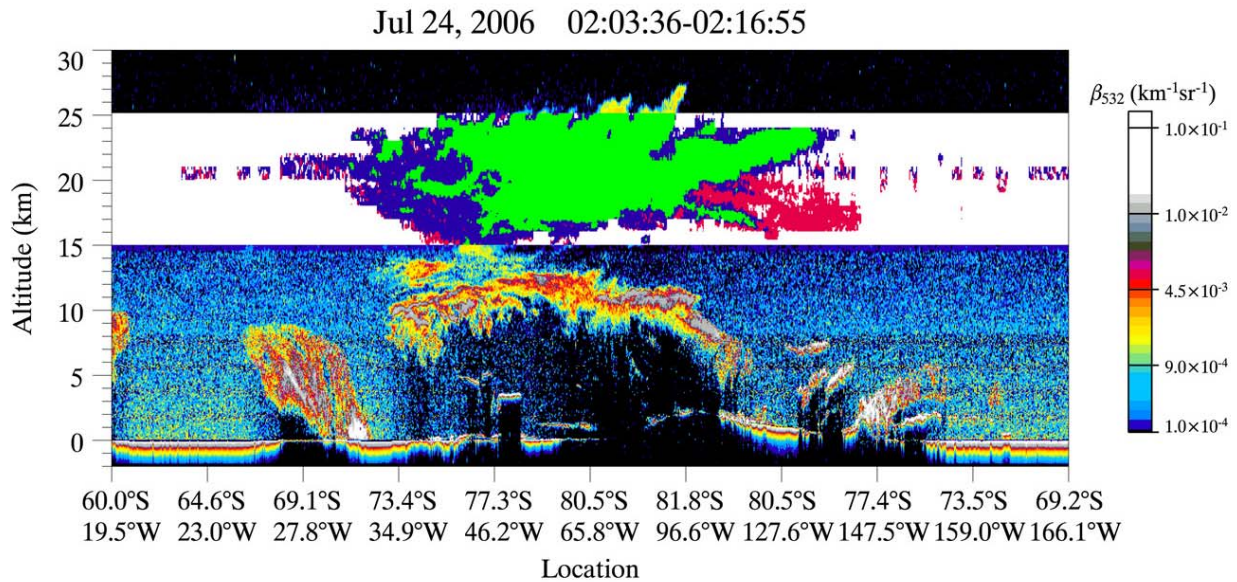
Figure 6. *Classification of PSC by composition for the same orbital section of CALIPSO as in Figure 4. A median smoothing was applied to the data prior to classification. Between 15 – 25 km, the color blue indicates type 1a, red indicates type 1b, and green indicates type 2 PSC.*

PSC occurrence over the Arctic region during the 2006 – 2007 winter (not shown) was much less frequent and the PSCs were optically thinner. Since temperatures in the Arctic winters tend to be generally warmer and more variable than those in the Antarctic winters as a result of higher atmospheric wave activity in the northern

7

hemisphere (Solomon, 1999), this result is not surprising.

5. SUMMARY.

In our study we used the 5 km horizontal layer CALIOP cloud product to analyze the latitude-longitude distribution of the cirrus cloud occurrence frequencies and thicknesses from June 2006 to June 2007. Our investigation of the top-level (single-layer) cirrus clouds showed maximum occurrence frequencies of up to 70% near the tropics over the 100° - 180° E longitude band. We also studied the seasonal variation of the horizontal distribution of cirrus cloud occurrence frequency and our results showed large latitudinal movement of cirrus cloud cover with the changing seasons, which is in agreement with previous studies (Wang et al., 1996; Wylie and Menzel, 1999). Our investigation of cirrus thickness occurrence frequency showed that the average thickness of cirrus clouds was generally between 1.5 and 1.9 km in the majority of latitude – longitude bins.

A PSC classification algorithm based on several other optical parameters is being explored. In this case, the most important linear combinations of the optical parameters are being identified using a linear principal component analysis, and the reduced optical parameter dataset will be separated into different categories based on a clustering algorithm.

We also plan to continue our quest for the construction of a cirrus cloud climatology as more and more data become available using the unique opportunity provided by CALIPSO.

6. REFERENCES.

Browell, E. V., S. Ismail, A. F. Carter, N. S. Higdon, C. F. Butler, P. A. Robinette, O. B. Toon, M. R. Schoeberl, and A. F. Tuck, 1990: Airborne lidar observations in the wintertime Arctic Stratosphere: Polar stratospheric clouds. *Geophys. Res. Lett.*, *17*, 385-388.

Dessler, A. E., and P. Yang, 2003: The distribution of tropical thin cirrus clouds inferred from Terra MODIS data. *J. Clim.*, *16*, 1241–1248.

Dessler, A. E., S. P. Palm, W. D. Hart, and J. D. Spinhirne, 2006: Tropopause-level thin cirrus coverage revealed by ICESat/Geoscience Laser Altimeter System. *J. Geophys. Res.*, *111*, D08203, doi:10.1029/2005JD006586.

Eguchi, N., T. Yokota, and G. Inoue, 2007: Characteristics of cirrus clouds from ICESat/GLAS observations, *Geophys. Res. Lett.*, *34*, L09810, doi:10.1029/2007GL029529.

Hansen, J., M. Sato, and R. Ruedy, 1997: Radiative forcing and climate response, *J. Geophys. Res., 102*, 6831–6864.

Hostetler, C. A., Z. Liu, J. Reagan, M. Vaughan, D. Winker, M. Osborn, W. H. Hunt, K. A. Powell, and C. Trepte, 2006: CALIOP Algorithm Theoretical Basis Document: Calibration and Level 1 Data Products, PC-SCI-201, NASA Langley Research Center, Hampton, VA.

Liou, K. N., 1986: Influence of cirrus clouds on weather and climate processes: A global perspective. *Mon. Weather Rev.*, *114*, 1167–1198.

McCormick, M. P., 1987: SAGE II: An overview. *Adv. Space. Res.*, *7*, 219-226.

McCormick, M. P., 2004: Space Lidar for Earth and Planetary Missions. *ILRC 2004*, Proceedings of the Conference held 12-16 July, 2004 in Matera, Italy, ESA SP-561. Paris: European Space Agency.

McCormick, P., T. Kovacs, and C. Hostetler, 2002: CALIPSO Polar Stratospheric Cloud and Stratospheric Aerosol Measurements. *ILRC 2002*, Quebec City, Quebec.

McCormick, M. P., H. M. Steele, P. Hamill, W. P. Chu, and T. J. Swissler, 1982: Polar stratospheric cloud sightings by SAM II. *J. Atmos. Sci.*, *39*, 1387-1397.

Pitts, M. C., L. W. Thomason, L. R. Poole, and D. M. Winker, 2007: Characterization of Polar Stratospheric Clouds with Space-Borne Lidar: CALIPSO and the 2006 Antarctic Season. *Atmos. Chem. Phys. Discuss.*, *7*, 7933-7985.

Poole, L. R., and M. P. McCormick, 1988: Polar stratospheric clouds and the Antarctic ozone hole. *J. Geophys. Res.*, *93*, 8423-8430.

Rossow, W. B., and R. A. Schiffer, 1999: Advances in understanding clouds from ISCCP. *Bull. Amer. Meter. Soc., 80,* 2261– 2286.

Solomon, S., 1999: Stratospheric ozone depletion: A review of concepts and history. *Rev. Geophys.*, *37*, 275-316.

Solomon, S., R. R. Garcia, F. S. Rowland, and D. J. Wuebbles, 1986: On the depletion of Antarctic ozone. *Nature*, *321*, 755-758.

Spinhirne, J. D., S. P. Palm, W. D. Hart, D. L. Hlavka, and E. J. Welton, 2005: Cloud and aerosol measurements from GLAS: Overview and initial results. *Geophys. Res. Lett.*, *32*, L22S03, doi:10.1029/2005GL023507.

Starr, D. O'C, 1987: A cirrus-cloud experiment: Intensive field observations planned for FIRE. *Bull. Amer. Meteor. Soc., 68*, 119-124.

Toon, O. B., P. Hamill, R. P. Turco, and J. Pinto, 1986: Condensation of HNO_3 and HCl in the winter polar stratospheres. *Geophys. Res. Lett.*, *13*, 1284-1287.

Toon, O. B., S. Kinne, E. V. Browell, and J. Jordan, 1990: An analysis of lidar observations of polar stratospheric clouds. *Geophys. Res. Lett.*, *17*, 393-396.

Toon, O. B., and R. C. Miake-Lye, 1998: Subsonic aircraft: Contrail and cloud effects special study (SUCCESS), *Geophys. Res. Lett., 25*, 1109-1112.

Wang, P. H., P. Minnis, M. P. McCormick, G. S. Kent, and K. M. Skeens, 1996: A 6-year climatology of cloud occurrence frequency from stratospheric aerosol and gas experiment II observations (1985–1990). *J. Geophys. Res.*, *101*, 29,407–29,429.

Winker, D. M., J. Pelon, and M. P. McCormick, 2003: The CALIPSO mission: Spaceborne lidar for observation of aerosols and clouds, *Proc. SPIE*, *4893*, 1-11.

Woodbury, G. E., and M. P. McCormick, 1983: Global distributions of cirrus clouds determined from SAGE data. *Geophys. Res. Lett., 10,* 1180–1193.

Woodbury, G. E., and M.P. McCormick, 1986: Zonal and geographical distributions of cirrus clouds determined from SAGE data. *J. Geophys. Res.*, *91*, 2775 – 2785.

Wylie, D. P., and W. P. Menzel, 1999: Eight year of high cloud statistics using HIRS. *J. Climate*, *12*, 170–184.

Wylie, D. P., W. P. Menzel, H. M. Wolf, and K. I. Strabala, 1994: Four years of global cirrus cloud statistics using HIRS. *J. Climate*, *7*, 1972–1986.